I&EC research
Industrial & Engineering Chemistry Research

Article

pubs.acs.org/IECR

Scalable Preparation of Gd_2O_3:Yb^{3+}/Er^{3+} Upconversion Nanophosphors in a High-Gravity Rotating Packed Bed Reactor for Transparent Upconversion Luminescent Films

Jingning Leng,[†,‡] Jingyi Chen,[§] Dan Wang,*[,†] Jie-Xin Wang,[†] Yuan Pu,*[,‡] and Jian-Feng Chen[†,‡]

[†]Beijing Advanced Innovation Center for Soft Matter Science and Engineering, State Key Laboratory of Organic−Inorganic Composites, Beijing University of Chemical Technology, Beijing 100029, China

[‡]Research Centre of the Ministry of Education for High Gravity Engineering and Technology, Beijing University of Chemical Technology, Beijing 100029, China

[§]Andrews Osborne Academy, Willoughby, Ohio 44094, United States

ABSTRACT: Optically transparent upconversion luminescent organic−inorganic nanocomposites are of great significance in many fields. The related key science problems are how to control size and uniformity of upconversion nanophosphors, as well as the dispersity of the upconversion nanophosphors in transparent polymer matrix. In this article, we reported a novel route to prepare Gd_2O_3:Yb^{3+}/Er^{3+} nanophosphors by high gravity reactive precipitation along with post hydrothermal and calcination process. A rotating packed bed (RPB) reactor was used to create a high-gravity environment for intensified mixing during the precipitation process of particles. The as-prepared Gd_2O_3:Yb^{3+}/Er^{3+} nanoparticles exhibited uniform particle size of <100 nm, which is much smaller than the common route (~350 nm). After surface modification, they were also homogeneously mixed with commercial polyurethane (PU), forming flexible transparent composites. The transparent film of Gd_2O_3:Yb^{3+}/Er^{3+}-PU showed bright visible luminescence under near-infrared light irradiation, promising for upgrades of photovoltaic, photocatalysis, and wearable optoelectronics.

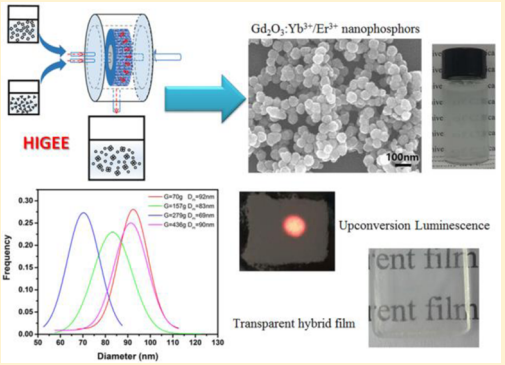

INTRODUCTION

Luminescent nanoparticles, including semiconductor quantum dots,[1] organic nanomicelles/nanodots,[2−4] metal nanoparticles,[5] carbon nanomaterials,[6,7] and rare-earth doped upconversion nanophosphors (UCNPs),[8−10] have received intense scientific attention and offer promising applications in many fields from optoelectronic devices to cancer treatment. Among them, UCNPs, which convert low energy near-infrared (NIR) light to high-energy ultraviolet or visible light, are of particular interest.[11] The unique property of UCNPs makes it possible to modify the solar spectrum to make it match better with the absorption spectrum of solar cells and therefore enhance the energy conversion efficiency solar cells. In theory, the standard AM1.5 spectrum power conversion efficiency of a single-bandgap solar cell can be increased by up to 50.7% by the application of an ideal upconverter.[12] Due to the different upconversion luminescence mechanism of UCNPs, it would be used in security or flexible transparent displays, if it can be dispersed in different kinds of polymers to form flexible transparent composites or transparent films.[13−16]

Gadolinium oxide (Gd_2O_3) has been widely used as a host in upconversion luminescence process due to its high chemical/thermal stability and lower phonon energy (phonon cutoff ~600 cm^{-1}),[17] as well as appropriate lattice matching with rare-earth ions (Yb^{3+}, Er^{3+}, Tm^{3+}, and Ho^{3+}) for upconversion phenomenon.[18] Meanwhile, the Gd also exhibits magnetic properties to fabricate optically and magnetically active bifunctional materials for advanced multifunctional devices.[19,20]

Therefore, the development of robust mass-scale synthesis methods for ultrafine rare-earth doped Gd_2O_3 particles is one of the key materials challenges in moving toward UCNPs for commercialization and advanced applications.

The rotating packed bed (RPB) reactor has been demonstrated as an efficient tool for process intensification during the preparation of nanoparticles.[21,22] The RPB can generate a high-gravity environment with homogeneous concentration, temperature, and supersaturation, which is of benefit for the homogeneous nucleation and growth of particles. In recent years, a variety of inorganic and organic nanoparticles with ultrafine size and uniform distribution have been prepared in high-gravity RPB reactors due to the intensified mixing and mass transfer, offering a very promising industrial platform for the production of nanomaterials.[23−27]

Received: June 1, 2017
Revised: June 19, 2017
Accepted: June 28, 2017
Published: June 28, 2017

DOI: 10.1021/acs.iecr.7b02262
Ind. Eng. Chem. Res. 2017, 56, 7977−7983

However, as far as we are aware, the process intensification studies of producing ultrafine UCNPs by RPB reactors have been rarely reported.

Herein, for the first time, we report a novel route to prepare ultrafine Gd_2O_3:Yb^{3+}/Er^{3+} upconversion nanophosphors by high-gravity intensified mixing in a RPB reactor with detailed studies on the effects of operating parameters, with a traditional stirred tank reactor (STR) adopted for comparison study. The morphologies, crystal structures, and surface properties of the obtained Gd_2O_3:Yb^{3+}/Er^{3+} nanoparticles were investigated by scanning electronic microscopy (SEM), powder X-ray diffraction (XRD), and Fourier transform infrared (FTIR) spectrophotometry. The upconversion luminescence of the Gd_2O_3:Yb^{3+}/Er^{3+} nanoparticles under excitation of a 980 nm near-infrared laser was observed and measured by spectra analysis. After surface modification, they were also homogeneously mixed with commercial polyurethane (PU), forming flexible transparent composites. The transparent film of Gd_2O_3:Yb^{3+}/Er^{3+}-PU showed bright visible luminescence under near-infrared light irradiation, promising for upgrades of photovoltaic, photocatalysis, and wearable optoelectronics.

EXPERIMENTAL SECTION

Materials. Gadolinium nitrate hexahydrate (GdN_3O_9·$6H_2O$), ytterbium nitrate pentahydrate (YbN_3O_9·$5H_2O$), and erbium trinitrate pentahydrate (ErN_3O_9·$5H_2O$) were purchased from Macklin Biochemical Co., Ltd. (Shanghai, China), whose purities were 99.9% metal basis. Urea was purchased from Sinopharm Chemical Reagent Co., Ltd. (Beijing, China) and anhydrous ethanol was purchased from Beijing Beihua Fine Chemicals Co., Ltd. (Beijing, China); both of them were analytical purity. All of the chemicals were used without any additional purification unless otherwise mentioned. Deionized water prepared by a Hitech Laboratory Water Purification System DW100 (Shanghai Hitech Instruments Co., Ltd.) was used for all experiments.

Synthesis of Gd_2O_3:Yb^{3+}/Er^{3+} Nanophosphors. The nanophosphors were synthesized by a well-developed urea-assisted homogeneous precipitation process.[28] In a typical synthesis approach shown in Figure 1a (i.e., flask experiment), $Gd(NO_3)_3$, $Yb(NO_3)_3$, $Er(NO_3)_3$, and urea were first formulated to 0.3, 0.02, 0.004, and 1.6 mol/L, respectively. Then 12.4 mL of $Gd(NO_3)_3$ aqueous solution, 10 mL of $Yb(NO_3)_3$ aqueous solution, and 10 mL of $Er(NO_3)_3$ aqueous solution (molar ratio of Gd, Yb and Er is 94:5:1) were mixed in a three-necked flask under vigorous stirring and added deionized water 100 mL to dilute. Then 75 mL of urea aqueous solution (molar ratio of urea and RE^{3+} ions is 30) was dropped into the above mixed solution slowly under vigorous stirring. After stirring for 15 min, the mixed solution was heated at 90 °C for 2 h. As the solution cooled to room temperature, the white precipitate was separated by centrifugation and washed 4 times with deionized water and anhydrous ethanol, respectively. Finally, the washed precipitate was annealed at 800 °C for 2 h in air atmosphere after drying at 80 °C for 6 h in vacuum oven, and Gd_2O_3:Yb^{3+}/Er^{3+} nanophosphors were obtained.

In order to investigate the effect of process intensification by high-gravity technology for the preparation of UCNPs, as schematically shown in Figure 1b (i.e., RPB experiment), a RPB reactor was used for the mixing the rare earth nitrates solution and the urea solution in the first step instead of mixing in a three-necked flask. The concentration and the volume of

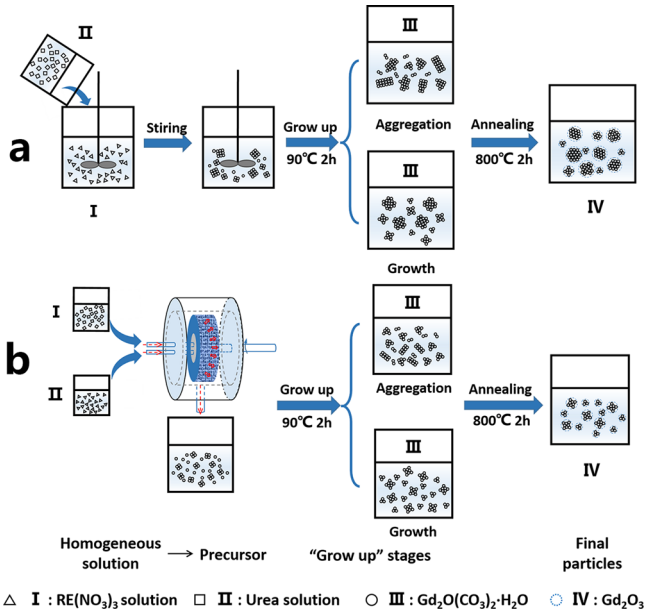

Figure 1. Schematic diagram of the routes for the preparation of Gd_2O_3:Yb^{3+}/Er^{3+} nanophosphors without (a) and with (b) high-gravity process intensification, respectively.

chemicals are the same as in the flask experiment. The mixture of 12.4 mL of 0.3 mol/L $Gd(NO_3)_3$ aqueous solution, 10 mL of 0.02 mol/L $Yb(NO_3)_3$ aqueous solution, 10 mL of 0.004 mol/L $Er(NO_3)_3$ aqueous solution (molar ratio of Gd, Yb and Er is 94:5:1), and 100 mL of deionized water was used as one feed. The 75 mL of 1.6 mol/L urea aqueous solution (molar ratio of urea and RE^{3+} ions is 30) was used as a second feed. The three-necked flask procedures are the same as the flask experiment. The RPB reactor consists of a rotator with stainless packing, a casing, two liquid inlets, an outlet, and a motor, and the detailed setup information on the RPB reactor can be found in previous reports.[22] In our experiments, we investigated the effects of different high gravity level factors on the sizes of the obtained nanophosphors by adjusting the rotation speeds of the RPB from 1000 to 2500 rpm. The relation between high gravity level and rotation speed will be explained later.

Preparation of Hydrophilic Gd_2O_3:Yb^{3+}/Er^{3+}@PEG Nanocomposites. The powders of the Gd_2O_3:Yb^{3+}/Er^{3+} were modified by polyethylene glycol 6000 (PEG-6000) to obtain hydrophilic Gd_2O_3:Yb^{3+}/Er^{3+}@PEG nanocomposites. Typically, 10 mg of the Gd_2O_3:Yb^{3+}/Er^{3+} powders were boiled in 40 mL of hydrogen peroxide (30 wt %) in a flask to introduce −OH groups onto the surface of the Gd_2O_3:Yb^{3+}/Er^{3+} until the remaining solution volume is 10 mL. 50 mL of deionized water were then added into the solution, and the mixture was cooled to room temperature. The precipitates were collected by centrifugation at 8000 rpm for 10 min to remove excess hydrogen peroxide and dispersed in 20 mL of 0.3 wt % PEG-6000 aqueous solution under stirring at room temperature for 3 h. The Gd_2O_3:Yb^{3+}/Er^{3+}@PEG nanocomposites were then collected by centrifugation at 8000 rpm for 10 min and dried at 180 °C for 6 h in a vacuum oven.

Characterization. The morphology studies were performed using a JEOL JSM-6360LV scanning electron microscope (SEM). The particle size distributions of the samples (diameter) were measured from SEM photographs using the ImageJ software. For each sample, over 200 particles from different images taken from various areas of the sample were

DOI: 10.1021/acs.iecr.7b02262
Ind. Eng. Chem. Res. 2017, 56, 7977−7983

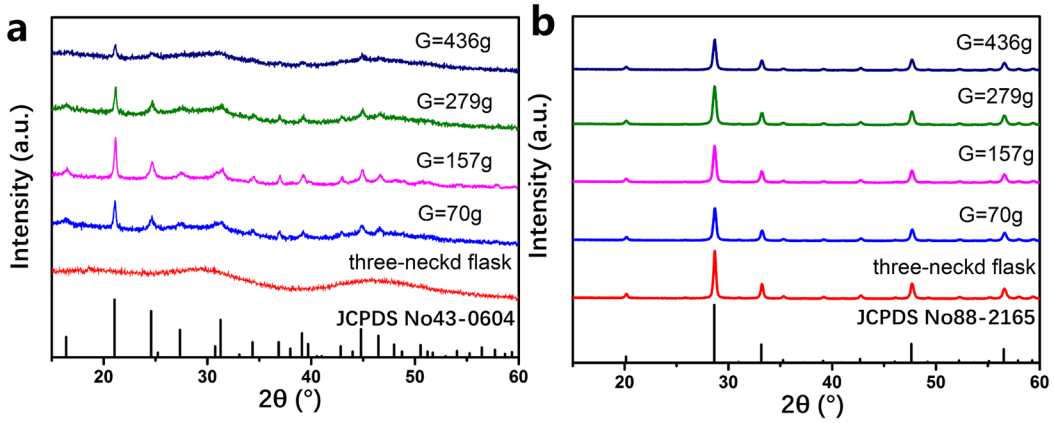

Figure 2. (a) XRD patterns of (a) intermediate and (b) final products of Gd_2O_3:Yb^{3+}/Er^{3+} nanophosphors.

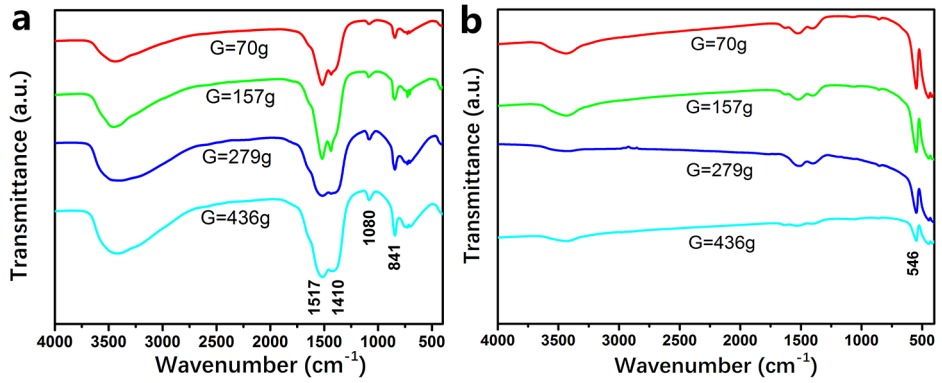

Figure 3. FTIR spectra of (a) unannealed powers and (b) annealed Gd_2O_3:Yb^{3+} /Er^{3+} nanoparticles.

considered for analysis. A typical transmission electron microscopic (TEM) image of the UCNPs in the hybrid film was taken using a Hitachi H-9500 TEM working in bright-field mode. X-ray diffraction (XRD) patterns of the samples were measured by an XRD-6000 diffractometer (Shimadzu Inc.). A PerkinElmer spectrum GX Fourier transform infrared (FTIR) spectroscopy system was used to record the FITR spectra of solid samples. Thermogravimetric analysis (TGA) was performed by using a Q50 TGA from TA Instruments. Upconversion luminescence spectra of the sample were acquired on a Maestro in vivo optical imaging system (CRI, Inc. Woburn, MA) equipped with a commercial 980 nm laser.

RESULTS AND DISCUSSION

The main focus of this work was to investigate the effect of high-gravity process intensification on the preparation of spherical Gd_2O_3:Yb^{3+}/Er^{3+} nanophosphors via a urea-assisted homogeneous precipitation process. The high gravity level G, which refers to the ratio of the average high gravitational acceleration in the RPB to the gravitational acceleration, plays a critical role in the mass transfer process of the RPB reactor. The high gravity level of the RPB could be calculated by the following equation. More information could be seen in our previous papers.[22,29] According to the following equations, the high gravity level is only related to the rotor speed, in the case of using the same setup of RPB.

$$G = \frac{\omega^2 r}{g}$$

$$r = \sqrt{\frac{r_1^2 + r_2^2}{2}}$$

In our experiments, four kinds of samples obtained via RPB routes at various rotation speeds (1000, 1500, 2000, and 2500 rpm, respectively) which correspond to the high gravity level G (70g, 157g, 279g, and 436g) were analyzed. The sample obtained by precipitation process in a flask was also prepared as a control. Figure 2a,b shows the XRD patterns of the intermediate products (i.e., unannealed powders) and final products of the Gd_2O_3:Yb^{3+}/Er^{3+} nanophosphors, respectively. It can be obviously observed that all of the diffraction peak positions of the intermediate products obtained in the RPB route were in good agreement with the International Center for Diffraction Data (ICDD) for $Gd_2O(CO_3)_2{\cdot}H_2O$ crystal (JCPDS: 43-0604). However, the sample obtained by mixing urea and $RE(NO_3)_3$ (RE = Gd, Yb, and Er) solutions in a three-necked flask showed a very low crystalline structure. The diffraction peaks of Gd_2O_3 at 20.142°, 28.635°, 33.184°, 47.636°, and 56.528°, which correspond to the crystal planes of (211), (222), (400), (440), and (622), respectively, were observed for all five kinds of samples (Figure 2b). The XRD patterns of the final products were in good agreement with the standard pattern of Gd_2O_3 (JCPDS: 88-2165), and no significant impurity peaks were observed, indicating that Yb^{3+} and Er^{3+} ions have embedded into the Gd_2O_3 host lattices successfully. The following reaction may occur.

$$(NH_2)_2CO(s) + H_2O(l) \xrightarrow{\Delta} CO_2(g) + 2NH_3(g)$$

DOI: 10.1021/acs.iecr.7b02262
Ind. Eng. Chem. Res. 2017, 56, 7977−7983

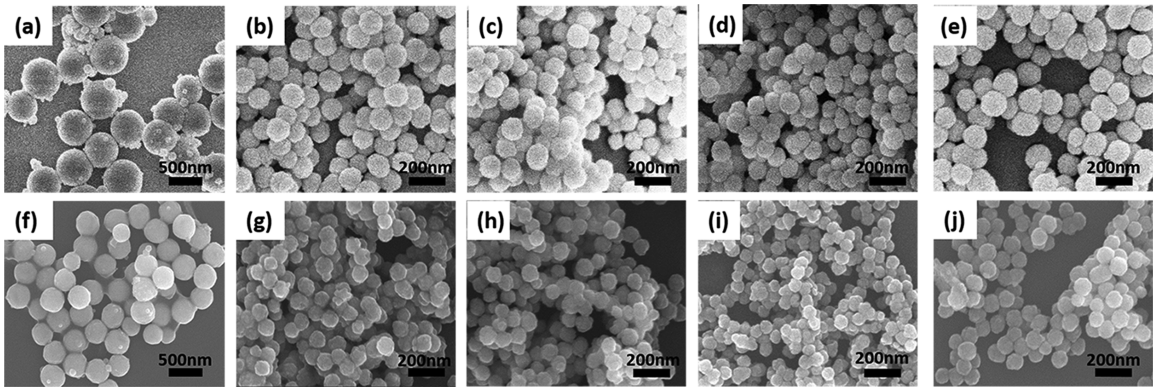

Figure 4. SEM images of (a) the unannealed sample synthesized a stirred tank reactor, (b–e) the unannealed sample using RPB with different high gravity level: 70g, 157g, 279g, and 436g, respectively. SEM images of (f–j) annealed Gd_2O_3:Yb^{3+}/Er^{3+} nanophosphors, whose preparation conditions are corresponding to (a–e) samples' preparation conditions.

$$CO_2(g) + H_2O(l) \rightarrow H_2CO_3(aq)$$

$$NH_3(g) + H_2O(l) \rightarrow NH_3{\cdot}H_2O(aq)$$

$$2Gd(NO_3)_3(aq) + 2H_2CO_3(aq) + 2NH_3{\cdot}H_2O(aq) \xrightarrow{\Delta} Gd_2O(CO_3)_2{\cdot}H_2O(s) + 2NH_4NO_3(aq) + 4HNO_3(aq)$$

$$Gd_2O(CO_3)_2{\cdot}H_2O(s) \xrightarrow{\Delta} Gd_2O_3(s) + H_2O(l) + 2CO_2(g)$$

Figure 3 shows the FTIR spectra of intermediate and final products of Gd_2O_3:Yb^{3+}/Er^{3+} nanoparticles. Free carbonate ions have four kinds of vibration absorption frequencies; two of them near 1063 and 879 cm^{-1} are nondegenerate.[30] The degenerate peak near 1415 and 700 cm^{-1} could be split into two absorption peaks during the formation of salt substances.[31] Figure 3a shows the FTIR spectra of the unannealed powders with different experiment processes and different high gravity levels, which confirms that the unannealed samples have carbonate ions, while no absorption peaks of free carbonate ions were observed from annealed powders of Gd_2O_3:Yb^{3+}/Er^{3+} nanophosphors (Figure 3b). In addition, strong absorption peaks at 546 and 444 cm^{-1} appear in FTIR spectra of Gd_2O_3:Yb^{3+}/Er^{3+}, which were associated with the vibration of the Gd–O bond, demonstrating the formation of Gd_2O_3 particles.[32]

Figure 4 shows the SEM images of the five kinds of samples before (a–e) and after (f–j) annealing at 800 °C. It was noted that the particle sizes have no obvious change before and after the annealing processing, demonstrating that the homogeneous precipitation process of urea and $RE(NO_3)_3$ (RE = Gd, Yb, and Er) solutions plays a decisive role in the size distribution of the final Gd_2O_3:Yb^{3+}/Er^{3+} nanophosphors. The particles obtained by mixing in the flask (Figure 3a,f) showed an average size of 350 nm, which was coincident with those given in the literature.[28] However, due to the high-gravity field in the RPB, the liquids going through the packing are spread or split into very fine droplets, threads, and thin films in the porous packing and the mass transfer and micromixing can be intensified greatly.[33,34] The particles obtained by mixing in RPB reactors (Figure 3b–e and g–j) exhibited much smaller sizes than those obtained in the flask. The morphology shows the sphere nanoparticles with a uniform size distribution for each sample.

The size distribution profiles of annealed Gd_2O_3:Yb^{3+}/Er^{3+} nanoparticles obtained by RPB routes are presented in Figure 5.

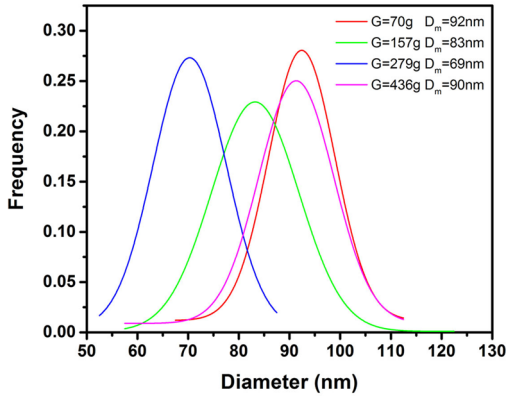

Figure 5. Size distribution profiles of annealed Gd_2O_3:Yb^{3+}/Er^{3+} nanoparticles obtained by RPB routes with different high gravity levels.

The particle sizes were 92, 83, 69, and 90 nm or the high gravity level of 70g, 157g, 279g, and 436g, respectively, inferring that the high gravity level of the RPB has influenced the size of the particle. The typical element mapping of Gd_2O_3:Yb^{3+}/Er^{3+} nanoparticles shown in Figure 6 indicated that the relative contents of doped ytterbium and erbium are uniformly distributed within the sample Gd_2O_3 nanoparticles.

It was noted that, when the high gravity level was 436g, the crystallinity of intermediate product (Figure 1a) decreases and final particle size (Figures 4 and 5) increases, which were not consistent with the overall trend. We consider that the high-gravity rotating packed bed intensified reaction has a suitable high gravity level. At the suitable high gravity level, the enhancement effect is obvious; once beyond the range, the enhancement effect will be relatively reduced. When the high gravity level was 436g, because the level is too high, the residence time of the solution in the high-gravity rotating packed bed is too short to form the uniform and stable nucleation,and the crystallinity of the intermediate product decreases and final particle size increases.

Figure 7a shows a typical upconversion luminescence spectrum of Gd_2O_3:Yb^{3+}/Er^{3+} nanophosphors under the excitation of a 980 nm laser. The sample exhibits two main

DOI: 10.1021/acs.iecr.7b02262
Ind. Eng. Chem. Res. 2017, 56, 7977–7983

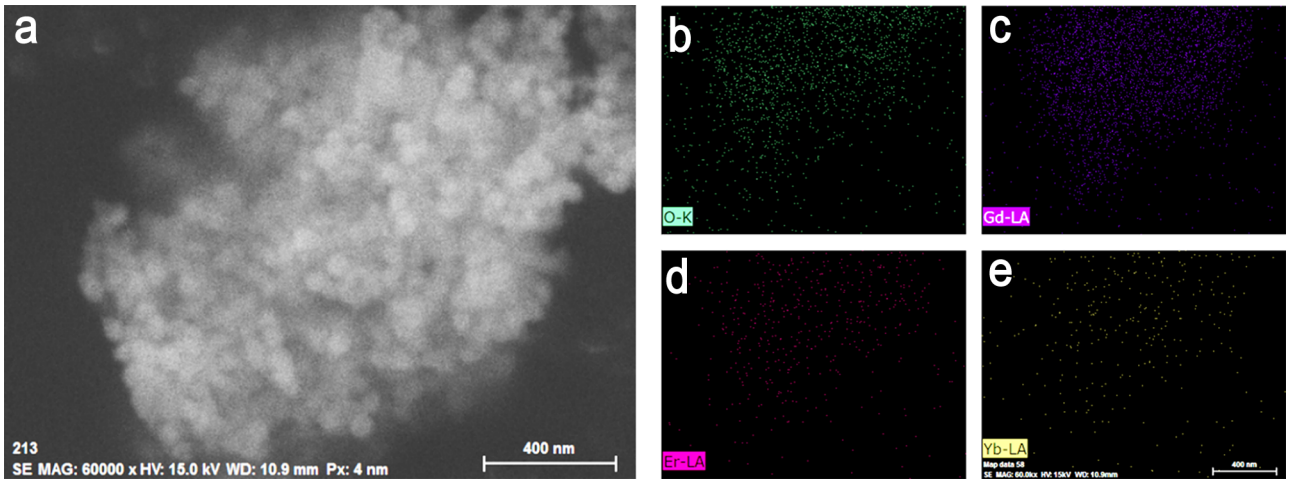

Figure 6. Element mapping of Gd_2O_3:Yb^{3+}/Er^{3+} nanophosphors. (a) SEM image, (b) O mapping, (c) Gd mapping, (d) Er mapping, and (e) Yb mapping.

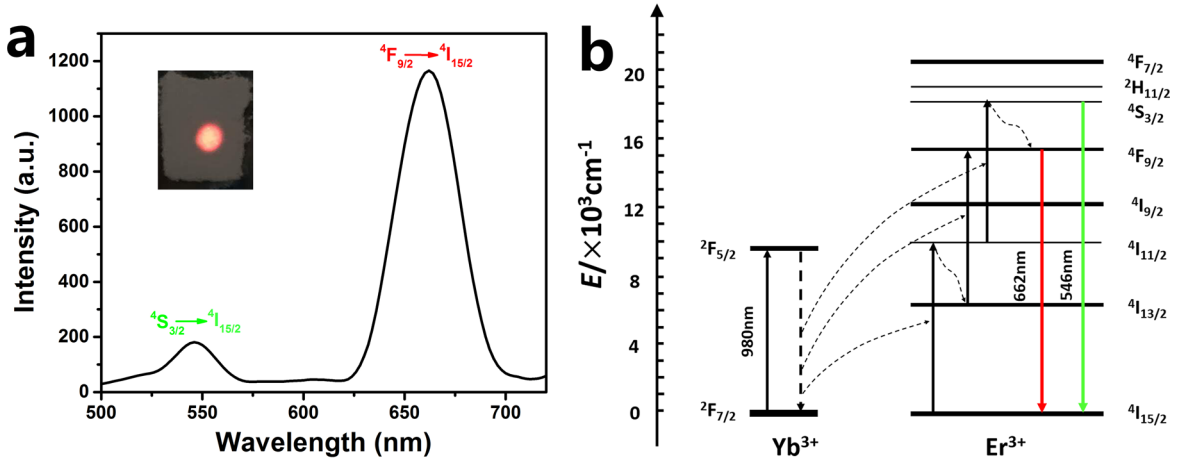

Figure 7. (a) Typical upconversion luminescence spectrum of Gd_2O_3:Yb^{3+}/Er^{3+} nanophosphors nanophosphors excited by a 980 nm optical laser. (b) Energy level diagrams of Yb^{3+} and Er^{3+} ions and the probable upconversion mechanism under the excitation of 980 nm light.

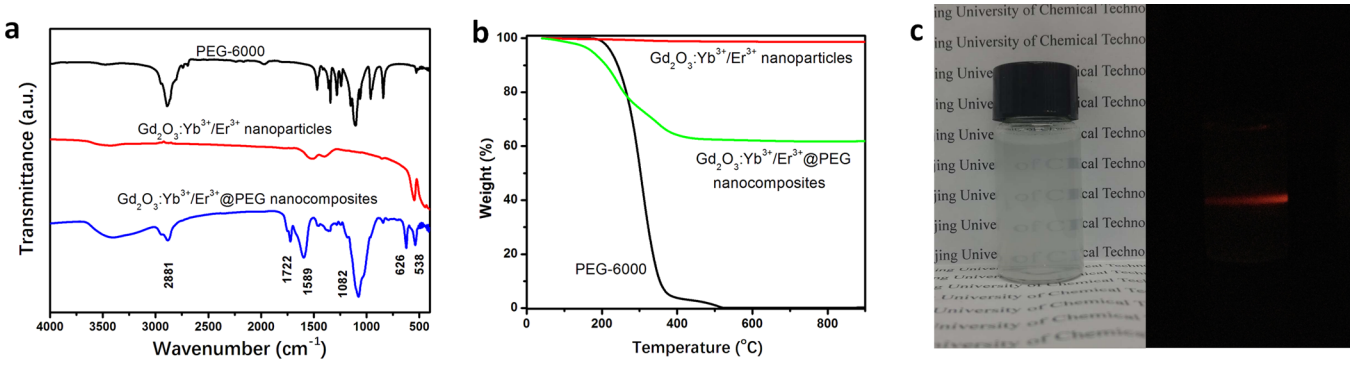

Figure 8. (a) FTIR spectra and (b) TGA results of PEG-6000, Gd_2O_3:Yb^{3+}/Er^{3+} nanoparticles, and Gd_2O_3:Yb^{3+}/Er^{3+}@PEG nanocomposites; (c) aqueous dispersion of Gd_2O_3:Yb^{3+}/Er^{3+}@PEG (0.1 mg/mL) under daylight and excited by a 980 nm laser.

upconversion emission bands in the visible spectrum, including a strong red emission band at around 662 nm and a relatively weak green emission band at around 546 nm, which correspond to the $^4F_{9/2} \rightarrow {}^4I_{15/2}$ and $^4S_{3/2} \rightarrow {}^4I_{15/2}$ transitions of Er^{3+} ions, respectively.[35] The inset in Figure 7a shows a picture of Gd_2O_3:Yb^{3+}/Er^{3+} powders under a 980 nm laser excitation, exhibiting bright red luminescence. Figure 7b shows the energy level diagrams of Yb^{3+} and Er^{3+} ions and the probable upconversion luminescence mechanism of the sample under the excitation of 980 nm, which involves several processes such as ground state absorption (GSA), excited state absorption (ESA), energy transfer (ET) process, and nonradiative relaxation (NR).[36] When the product was excited by 980 nm optical fiber laser, Er^{3+} ions on the ground state ($^4I_{15/2}$) are excited to $^4I_{11/2}$, where the energy comes from the GSA by itself and/or ET from Yb^{3+} to Er^{3+}, first. Then a part of the excited

DOI: 10.1021/acs.iecr.7b02262
Ind. Eng. Chem. Res. 2017, 56, 7977−7983

electrons on the $^4I_{11/2}$ level will populate the intermediate level $^4I_{13/2}$ by NR process, and other excited electrons on the $^4I_{11/2}$ level will continue to absorb energy and populate $^4S_{3/2}$ by ESA and/or second-step ET from Yb^{3+} to Er^{3+}. After that, the electrons on the intermediate level $^4I^{13/2}$ are further excited into $^4F_{9/2}$ by ESA and a part of electrons on the $^4S_{3/2}$ will populate $^4F_{9/2}$ by NR. Finally, the $^4S_{3/2}$ level undergoes radiative decay to produce green emission (546 nm), and the $^4F_{9/2}$ level undergoes radiative decay to produce red emission (662 nm).

Figure 8a shows the FTIR spectra of Gd_2O_3:Yb^{3+}/Er^{3+} nanophosphors before and after modification by PEG-6000. The PEG modified Gd_2O_3:Yb^{3+}/Er^{3+} nanoparticles showed a symmetric stretching vibration peak of $-CH_2-$ near 2881 cm^{-1}, the peak of hydrogen bonding between −OH near 1600 cm^{-1}, and the vibration peak of −C−O−C− near 1100 cm^{-1}, which confirms that the PEG-6000 was combined successfully with Gd_2O_3:Yb^{3+}/Er^{3+} nanophosphors. The weight ratio of Gd_2O_3:Yb^{3+}/Er^{3+} and PEG-6000 in the Gd_2O_3:Yb^{3+}/Er^{3+}@PEG hybrid nanocomposites was 3:1, determined by TGA analysis which was obtained in air atmosphere (Figure 8b). Figure 8c shows the hydrophilic Gd_2O_3:Yb^{3+}/Er^{3+}@PEG dispersion in water (0.1 mg/mL), and the luminescence picture under a 980 nm laser excitation, in which a bright red line was observed due to the upconversion luminescence and Tyndall effect of the Gd_2O_3:Yb^{3+}/Er^{3+} dispersion.

In order to explore the potential functions and applications of Gd_2O_3:Yb^{3+}/Er^{3+} in polymer films, we choose to mix waterborne polyurethane (PU) and Gd_2O_3:Yb^{3+}/Er^{3+}@PEG into a transparent film. Figure 9 shows the pictures of a waterborne PU film and a Gd_2O_3:Yb^{3+}/Er^{3+}-PU hybrid film under daylight and 980 nm light, respectively. Transparent Gd_2O_3:Yb^{3+}/Er^{3+}-PU hybrid films were prepared by adding 0.2 wt % Gd_2O_3:Yb^{3+}/Er^{3+}@PEG into waterborne PU, while pure waterborne PU films were used as the reference. The size of the two kinds of films was 2 cm × 2 cm and the thickness was 2 mm. The letters under the films could be read clearly, which illustrates that both of the films have high transmission of visible light (Figure 9a). Meanwhile, the Gd_2O_3:Yb^{3+}/Er^{3+}-PU film showed red emission while no emission was observed from the pure waterborne PU film under 980 nm light (Figure 9b).

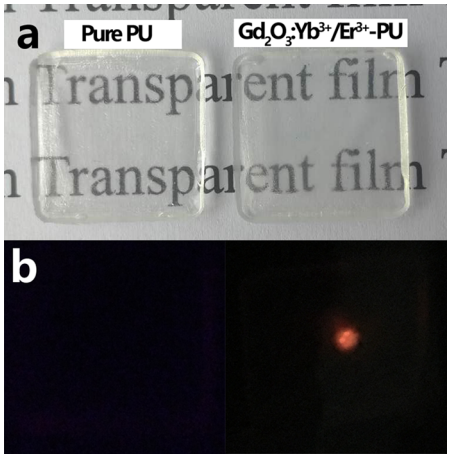

Figure 9. Digital photos of a pure waterborne PU film and a typical Gd_2O_3:Yb^{3+}/Er^{3+}-PU hybrid film (2 cm × 2 cm × 2 mm) under daylight (a) and 980 nm light (b), respectively.

Figure 10a shows the UV−visible transmittance spectra of the PU film and the UCNPs-PU hybrid film (with 2 wt % Gd_2O_3:Yb^{3+}/Er^{3+}@PEG) in the range of 200−800 nm, respectively. The PU film and the UCNPs-PU hybrid film exhibited similar transmittance spectra, indicating that the adding of Gd_2O_3:Yb^{3+}/Er^{3+}@PEG in the PU film caused no significant absorbance or scattering of visible light. A typical TEM image of UCNPs in PU hybrid films in Figure 10b showed the uniform distribution of UCNPs in the PU matrix, with no significant aggregates observed.

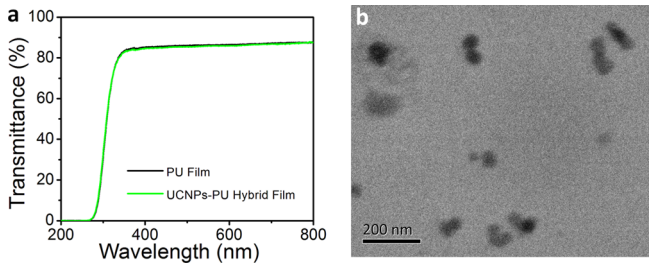

Figure 10. (a) UV−visible transmittance spectra of PU and UCNPs-PU hybrid films (with 2 wt % Gd_2O_3:Yb^{3+}/Er^{3+}@PEG) in the range of 200−800 nm; (b) a typical TEM image of UCNPs in PU hybrid films.

CONCLUSION

In conclusion, Gd_2O_3: Yb^{3+}/Er^{3+} upconversion nanophosphors were prepared by high gravity reactive precipitation along with a post hydrothermal and calcination process. The obtained Gd_2O_3: Yb^{3+}/Er^{3+} phosphors exhibited a particle size of <100 nm, which is much smaller than that from the common route (~360 nm), due to the intensified mixing by high-gravity rotating packed bed. After surface modification with PEG-6000, they were also homogeneously mixed with waterborne PU, forming flexible transparent composites. The transparent film of Gd_2O_3: Yb^{3+}/Er^{3+}-PU showed bright visible luminescence under near-infrared 980 nm light irradiation, promising for upgrades of photovoltaic, photocatalysis, and wearable optoelectronics.

AUTHOR INFORMATION

Corresponding Authors

*Tel: +86-10-64449453. E-mail: wangdan@mail.buct.edu.cn.
*Tel: +86-10-64421905. E-mail: puyuan@mail.buct.edu.cn.

ORCID

Dan Wang: 0000-0002-3515-4590
Jie-Xin Wang: 0000-0003-0459-1621

Funding

This work was supported by the National Key Research and Development Program of China (2017YFB0404302/2017YFB0404300), National Natural Science Foundation of China (51641201, 21620102007 and 21622601), the Fundamental Research Funds for the Central Universities (BUCTRC201601), and the "111" project of China (B14004).

Notes

The authors declare no competing financial interest.

REFERENCES

(1) Kairdolf, B. A.; Smith, A. M.; Stokes, T. H.; Wang, M. D.; Young, A. N.; Nie, S. M. Semiconductor Quantum Dots for Bioimaging and Biodiagnostic Applications. *Annu. Rev. Anal. Chem.* **2013**, *6*, 143−162.
(2) Yang, Y.; Wang, X. Y.; Cui, Q. L.; Cao, Q.; Li, L. D. Self-assembly of Fluorescent Organic Nanoparticles for Iron(III) Sensing and Cellular Imaging. *ACS Appl. Mater. Interfaces* **2016**, *8*, 7440−7448.

DOI: 10.1021/acs.iecr.7b02262
Ind. Eng. Chem. Res. 2017, 56, 7977−7983

(3) Wang, D.; Qian, J.; Qin, W.; Qin, A. J.; Tang, B. Z.; He, S. L. Biocompatible and Photostable AIE Dots with Red Emission for In Vivo Two-photon Bioimaging. *Sci. Rep.* **2015**, *4*, 4279.
(4) Kim, S.; Pudavar, H. E.; Bonoiu, A.; Prasad, P. N. Aggregation-enhanced Fluorescence in Organically Modified Silica Nanoparticles: A Novel Approach toward High-Signal-Output Nanoprobes for Two-Photon Fluorescence Bioimaging. *Adv. Mater.* **2007**, *19*, 3791−3795.
(5) Bigall, N. C.; Parak, W. J.; Dorfs, D. Fluorescent, Magnetic and Plasmonic-hybrid Multifunctional Colloidal Nano Objects. *Nano Today* **2012**, *7*, 282−296.
(6) Wang, D.; Chen, J. F.; Dai, L. M. Recent Advances in Graphene Quantum Dots for Fluorescence Bioimaging from Cells through Tissues to Animals. *Part. Part. Syst. Charact.* **2015**, *32*, 515−523.
(7) Mao, L. H.; Tang, W. Q.; Deng, Z. Y.; Liu, S. S.; Wang, C. F.; Chen, S. Facile Access to White Fluorescent Carbon Dots Toward Light-emitting Devices. *Ind. Eng. Chem. Res.* **2014**, *53*, 6417−6425.
(8) Liu, J.; Wu, R.; Li, N.; Zhang, X.; Zhan, Q.; He, S. Deep, High Contrast Microscopic Cell Imaging Using Three-Photon Luminescence of β-($NaYF_4$:Er^{3+}/$NaYF_4$) Nanoprobe Excited by 1480-nm CW Laser of Only 1.5-mW. *Biomed. Opt. Express* **2015**, *6*, 1857−1866.
(9) Zhan, Q.; Qian, J.; Liang, H.; Somesfalean, G.; Wang, D.; He, S.; Zhang, Z.; Andersson-Engels, S. Using 915 nm Laser Excited Tm^{3+}/Er^{3+}/Ho^{3+}-doped $NaYbF_4$ Upconversion Nanoparticles For *In Vitro* And Deeper *In Vivo* Bioimaging Without Overheating Irradiation. *ACS Nano* **2011**, *5*, 3744−3757.
(10) Zhan, Q.; Zhang, X.; Zhao, Y.; Liu, J.; He, S. Tens of Thousands-Fold Upconversion Luminescence Enhancement Induced by A Single Gold Nanorod. *Laser Photonics Rev.* **2015**, *9*, 479−487.
(11) Wang, D.; Zhu, L.; Chen, J. F.; Dai, L. M. Liquid Marbles Based on Magnetic Upconversion Nanoparticles as Magnetically and Optically Miniature Reactors for Photocatalysis and Photodynamic Therapy. *Angew. Chem., Int. Ed.* **2016**, *55*, 10795−10799.
(12) Zou, W. Q.; Visser, C.; Maduro, J. A.; Pshenichnikov, M. S.; Hummelen, J. C. Broadband Dye-sensitized Upconversion of Near-infrared Light. *Nat. Photonics* **2012**, *6*, 560−564.
(13) Watanabe, S.; Ishii, Y.; Soga, K.; Matsumoto, M. Calcination-free Micropatterning of Upconversion Luminescent Layers Consisting of Rare-earth-doped Ceramic Nanoparticles on Wettability-patterned Flexible Plastic Sheets by Soft-liquid Phase Adsorption. *Colloids Surf., A* **2016**, *506*, 210−219.
(14) Liu, H. C.; Jayakumar, MK. G.; Huang, K.; Wang, Z.; Zheng, X.; Ågren, H.; Zhang, Y. Phase Angle Encoded Upconversion Luminescent Nanocrystals for Multiplexing Applications. *Nanoscale* **2017**, *9*, 1676−1686.
(15) Watanabe, S.; Asanuma, T.; Sasahara, T.; Hyodo, H.; Matsumoto, M.; Soga, K. 3D Micromolding of Arrayed Waveguide Gratings on Upconversion Luminescent Layers for Flexible Transparent Displays without Mirrors, Electrodes, and Electric Circuits. *Adv. Funct. Mater.* **2015**, *25*, 4390−4396.
(16) Meruga, J.; Baride, A.; Cross, W.; Kellar, J.; May, P. S. Red-green-blue Printing Using Luminescence-upconversion Inks. *J. Mater. Chem. C* **2014**, *2*, 2221−2227.
(17) Tamrakar, R. K.; Bisen, D. P.; Upadhyay, K.; Sahu, I. P. Comparative Study and Role of Er^{3+} and Yb^{3+} Concentrations on Upconversion Process of Gd_2O_3: Er^{3+} Yb^{3+} Phosphors Prepared By Solid-state Reaction and Combustion Method. *J. Phys. Chem. C* **2015**, *119*, 21072.
(18) Guo, H.; Dong, N.; Yin, M.; Zhang, W. P.; Lou, L. R.; Xia, S. D. Visible Upconversion in Rare Earth Ion-doped Gd_2O_3 Nanocrystals. *J. Phys. Chem. B* **2004**, *108*, 19205−19209.
(19) Liu, Y. X.; Wang, D. S.; Shi, J. X.; Peng, Q.; Li, Y. D. Magnetic Tuning of Upconversion Luminescence in Lanthanide-doped Bifunctional Nanocrystals. *Angew. Chem., Int. Ed.* **2013**, *52*, 4366−4369.
(20) Zhou, J.; Yu, M. X.; Sun, Y.; Zhang, X. Z.; Zhu, X. J.; Wu, Z. H.; Wu, D. M.; Li, F. Y. Fluorine-18-labeled Gd^{3+}/Yb^{3+}/Er^{3+} Co-doped $NaYF_4$ Nanophosphors for Multimodality PET/MR/UCL Imaging. *Biomaterials* **2011**, *32*, 1148−1156.
(21) Rao, D. P.; Bhowal, A.; Goswami, P. S. Process Intensification in Rotating Packed Beds (HIGEE): An Appraisal. *Ind. Eng. Chem. Res.* **2004**, *43*, 1150−1162.
(22) Chen, J. F.; Wang, Y. H.; Guo, F.; Wang, X. M.; Zheng, C. Synthesis of Nanoparticles with Novel Technology: High-gravity Reactive Precipitation. *Ind. Eng. Chem. Res.* **2000**, *39*, 948−954.
(23) Sun, Q.; Chen, B.; Wu, X.; Wang, M.; Zhang, C.; Zeng, X. F.; Wang, J. X.; Chen, J. F. Preparation of Transparent Suspension of Lamellar Magnesium Hydroxide Nanocrystals Using a High-gravity Reactive Precipitation Combined with Surface Modification. *Ind. Eng. Chem. Res.* **2015**, *54*, 666−671.
(24) Ng, C. M.; Chen, P. C.; Manickam, S. Green High-gravitational Synthesis of Silver Nanoparticles Using a Rotating Packed Bed Reactor (RPBR). *Ind. Eng. Chem. Res.* **2012**, *51*, 5375−5381.
(25) Yang, Q.; Wang, J. X.; Guo, F.; Chen, J. F. Preparation of Hydroxyaptite Nanoparticles by Using High-gravity Reactive Precipitation Combined with Hydrothermal Method. *Ind. Eng. Chem. Res.* **2010**, *49*, 9857−9863.
(26) Chen, J. F.; Li, Y. L.; Wang, Y. H.; Yun, J.; Cao, D. P. Preparation and Characterization of Zinc Sulfide Nanoparticles Under High-gravity Environment. *Mater. Res. Bull.* **2004**, *39*, 185−194.
(27) Chen, J. F.; Shao, L.; Guo, F.; Wang, X. M. Synthesis of Nanofibers of Aluminum Hydroxide in Novel Rotating Packed Bed Reactor. *Chem. Eng. Sci.* **2003**, *58*, 569−575.
(28) Tian, Y.; Tian, B. N.; Cui, C. E.; Huang, P.; Wang, L.; Chen, B. J. Size-dependent Upconversion Luminescence and Temperature Sensing Behavior of Spherical Gd_2O_3: Yb^{3+}/Er^{3+} Phosphor. *RSC Adv.* **2015**, *5*, 14123−14128.
(29) Chen, J. F.; Shao, L. Mass Production of Nanoparticles by High Gravity Reactive Precipitation Technology with Low Cost. *China Particuol.* **2003**, *1*, 64−69.
(30) Fujita, J.; Martell, A. E.; Nakamoto, K. Infrared Spectra of Metal Chelate Compounds. VIII. Infrared Spectra of Co (III) Carbonato Complexes. *J. Chem. Phys.* **1962**, *36*, 339−345.
(31) Herzberg, G. Infrared and Raman Spectra of Polyatomic molecules. *Ann. Fac. Sci. Toulouse Sci. Math. Sci. Phys.* **1954**, 193−208.
(32) Garcıa-Murillo, A.; LeLuyer, C.; Dujardin, C.; Pedrini, C.; Mugnier, J. Elaboration and Characterization of Gd_2O_3 Waveguiding Thin Films Prepared by the Sol-gel Process. *Opt. Mater.* **2001**, *16*, 39−46.
(33) Yang, H. J.; Chu, G. W.; Zhang, J. W.; Shen, Z. G.; Chen, J. F. Micromixing Efficiency in a Rotating Packed Bed: Experiments and Simulation. *Ind. Eng. Chem. Res.* **2005**, *44*, 7730−7737.
(34) Chen, J. F.; Zheng, C.; Chen, G. A. Interaction of Macro- and Micromixing on Particle Size Distribution in Reactive Precipitation. *Chem. Eng. Sci.* **1996**, *51*, 1957−1966.
(35) Dong, H.; Sun, L. D.; Yan, C. H. Basic Understanding of the Lanthanide Related Upconversion Emissions. *Nanoscale* **2013**, *5*, 5703−5714.
(36) Mahata, M. K.; Kumar, K.; Rai, V. K. Structural and Optical Properties of Er^{3+} /Yb^{3+} Doped Barium Titanate Phosphor Prepared by Co-precipitation Method. *Spectrochim. Acta, Part A* **2014**, *124*, 285−291.

DOI: 10.1021/acs.iecr.7b02262
Ind. Eng. Chem. Res. 2017, 56, 7977−7983